Progress In Electromagnetics Research M, Vol. 64, 123–133, 2018

Breast Tumor Detection System Based on a Compact UWB Antenna Design

Ibtisam Amdaouch[1, *], Otman Aghzout[1, 2], Azzeddin Naghar[1, 3], Ana V. Alejos[3], and Francisco Falcone[4]

Abstract—This paper presents a novel breast model system based on a UWB antenna for locating a tumor cancer. The antenna with overall size of 35 mm × 20 mm × 1.6 mm is characterized with an ultra-wideband of 120% and frequency range of 3 GHz–12 GHz for the FCC band. The proposed antenna exhibits good impedance matching, high gain and omnidirectional radiation patterns. The measurement results are presented to illustrate the performances of the proposed antenna. This antenna has been implemented in a designed system model with dielectric properties of a human breast capable to detect strange objects. The size and localization coordinates of the tumor are studied in detail for better tumor detection. The coordinates of the corresponding maximum value of SAR are identified in order to accurately detect different locations of tumor inside the breast. The results show that the localization of the tumor can be detected with high precision which demonstrates the performance of the proposed antenna and the entire system. The proposed breast model system was developed using the commercial CST Microwave studio simulator.

1. INTRODUCTION

Breast cancer is the most common non-skin related malignancy and the second leading cause of cancer death among women in the world [1]. In 2014, an estimated 232,670 new cases of invasive breast cancer were expected to be diagnosed in women in the U.S., along with 62,570 new cases of non-invasive breast cancer as reported by the American Cancer Society, although some risk reduction might be achieved if they are detected in time. The current standard screening methods for detecting early stage breast cancer are X-ray mammography, ultrasound techniques and magnetic resonance imaging (MRI). The X-ray mammography is proved to be the most widely used and effective modality for early breast cancer detection. It is clinically employed as a regular screening method. Despite its successful detection results compared to other screening tools, X-ray mammography also has its drawbacks: its failure to distinguish between benign and malignant tumors, high false-alarm rate, discomfort to patients and difficulty to detect cancer in its initial formation state [2, 3]. All these limitations provide motivation and encouragement for the development of a complementary breast-imaging tool as an appealing alternative to the previous techniques. One of the various alternatives proposed is microwave imaging, in particular the ultra-wideband (UWB) frequency region. The principle that microwave imaging relies upon is the dielectric contrast between normal and cancerous human tissues [4]. The majority of the compact UWB antennas presented in the literature exhibit a large size with relatively low gain [5, 6], which is suitable for specific communications. In this paper, we present a new design of compact UWB antenna for breast tumor detection system. The rectangular ring shaped UWB antenna for breast imaging developed in this

Received 24 October 2017, Accepted 4 December 2017, Scheduled 8 February 2018

* Corresponding author: Ibtisam Amdaouch (amdaouch.ibtisam@gmail.com).

[1] Faculty of Sciences, National School of Applied Sciences, Abdelmalek Essaadi University, Tetouan, Morocco. [2] Electronics and Microwave Group, Telecommunication Department, ENSA, Tetouan, Morocco. [3] Signal Theory and Communication Department, University of Vigo, Pontevedra, Vigo, Spain. [4] Millimeter and Terahertz Waves Lab. UN, Pamplona, Spain.

paper has a planar type design with a high gain, compact size and relatively omnidirectional radiation patterns suitable for being placed directly on the target [5]. The antenna parameters such as return loss, gain, radiation pattern and current distribution are discussed in detail. The antenna is characterized by an ultra-wideband of 120% (3–12 GHz) and exhibits good gain and omnidirectional pattern. The prototype of the antenna for high frequencies can be found in our previous work [7]. It can be seen that the antenna is a good candidate for microwave imaging. As a second step, we design a tumor detection system with a breast model along with the proposed antenna. In fact in spite of research that shows the ability of microwave detection technology, there is a lack of realistic breast models for testing. Then, our breast model includes heterogeneities that are similar to a real breast and represents all the important dielectric structure described in the literature. The breast model with a skin layer of 2 mm and fat layer into the breast to get closer to reality are respectively considered. Detection capabilities provided by the whole system are also presented. The results show that the proposed detection system can achieve high accuracy with excellent performance.

2. BREAST CANCER DETECTION SYSTEM

2.1. System Design Description

In order to verify the validation of any imaging technique, a model representing the main tissues of the object under study is required. The principle of microwave imaging for breast cancer detection is based on the large contrast of the dielectric constant and conductivity between the malignant tumor and other breast tissues [8, 9]. In fact, a UWB microwave pulse is radiated by the antenna into the breast penetrating the skin and traveling through the breast to interact with the malignant and other breast tissues. The reflections occurring on the surface of these tissues are due to different characteristics of microwave absorption, reflection and transmission. As the breast tissues appear as lossy dispersive material to the microwave propagation, it is necessary to take the dispersive effect into account to approach the real electrical properties of the breast model. Their behaviour, to variation of frequency, is most likely to be governed by single-pole Debye model, expressed as follows:

$$\varepsilon_r(\omega) = \varepsilon_\infty + \frac{\varepsilon_s - \varepsilon_\infty}{1 + \omega^2\tau^2} \tag{1}$$

$$\sigma_r(\omega) = \frac{(\varepsilon_s - \varepsilon_\infty)\omega^2\tau\varepsilon_0}{1 + \omega^2\tau^2} + \sigma_s \tag{2}$$

where ε_r is the complex permittivity, ε_0 the permittivity of free space, ε_∞ the dielectric constant at infinite, ε_s the static(zero frequency) dielectric constant of the material, σ_s the static conductivity, τ the pole relaxation constant, and ω the angular frequency. In this paper, the most representative breast model developed by the Computational Electromagnetic Group of Wisconsin is considered [10]. The system is simulated using the commercial CST Microwave Studio simulator. In order to emulate the tumor realistic size, two values, 5 mm and 6 mm, are considered for the tumor radius. The 3-D view of the numerical abnormal breast model with the antenna developed in this work is illustrated in Figure 9. Both dielectric properties and tumor characteristics are shown in Table 1, where σ is the tissue conductivity and ε_r the relative permittivity.

Table 1. Dielectric property and conductivity of breast and tumor model.

	Conductivity σ	The relative permittivity ε_r
Skin	1.1	37
tumor	4	50

2.2. Antenna Design

For microwave imaging, the antenna is considered one of the most important component to provide significant efficiency of the entire system. The antenna for the detection cancer system proposed in

this paper has a square ring shape, with a compact size of 35 mm × 20 mm and a uniform strip width $w_f = 1.8$ mm providing an impedance matching for 50 Ω. The microstrip feed line used to feed the antenna is offset from the center. The antenna is printed on an FR-4 dielectric substrate, with a thickness of 1.6 mm and relative permittivity ε_r of 4.4. Moreover, a partial conducting ground plane of dimensions 8 mm × 20 mm has been used to improve the impedance matching of the antenna. Fig. 1 depicts the described structure. The optimized values of the antenna parameters are shown in Table 2.

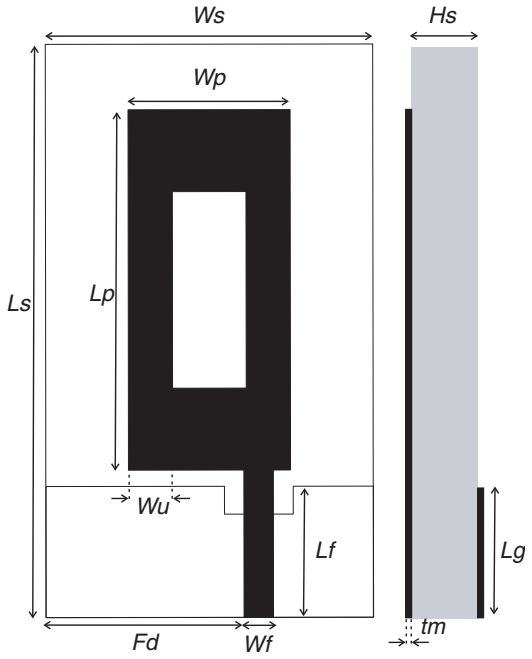

Figure 1. Square ring shape UWB antenna.

Table 2. Parameter value of the proposed antenna.

Parameter	Value (mm)
W_s	20
L_s	35
H_s	1.6
W_p	9.9
L_p	22
W_u	2.7
W_f	1.8
L_f	9
tm	9
Fd	12
L_g	8

3. ANTENNA PERFORMANCE

For further improvement in the bandwidth and return loss of the antenna, different feed positions were considered and studied. Fig. 2 depicts the resulting return loss response corresponding to different positions of the feedline, when all other parameters are kept constant. It is shown that shifting the

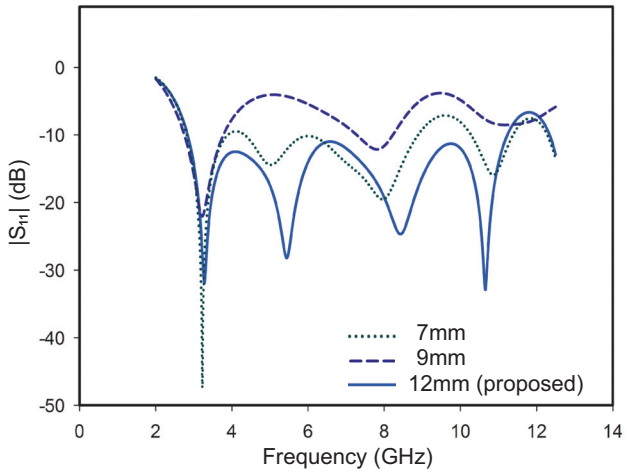

Figure 2. Return loss for different positions of the feedline.

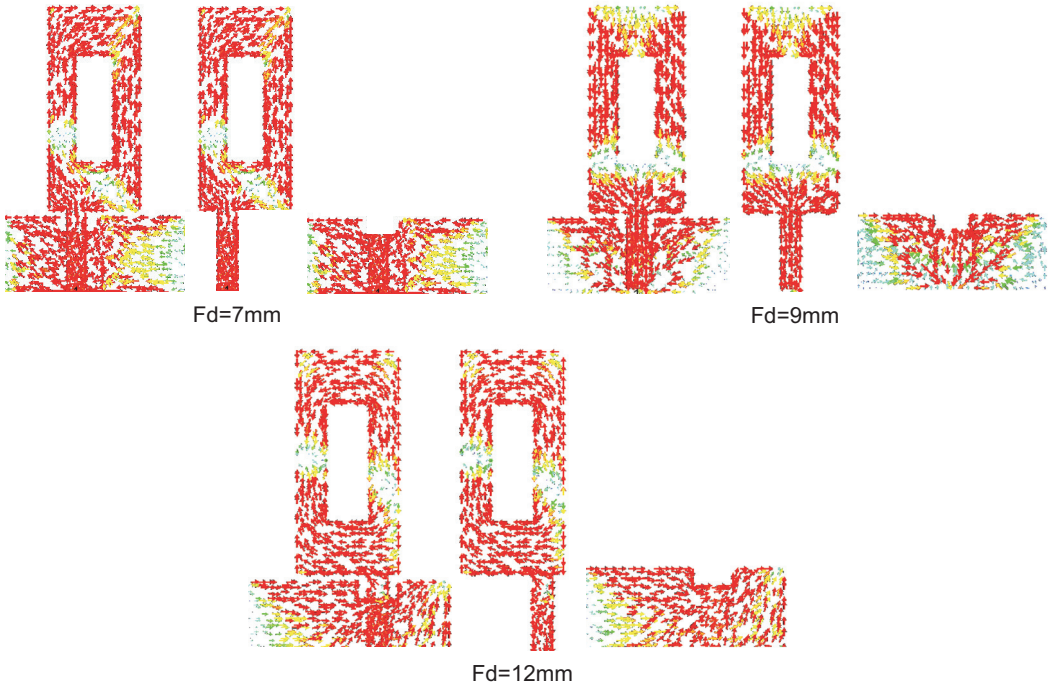

Figure 3. Current distribution for different positions of the feedline at 5.8 GHz.

feedline position by varying F_d around the reference position tends to have an ultrawide band response. In fact, the position of the feed at 12 mm extends the bandwidth from 2.9 GHz to 13 GHz [11, 12]. Fig. 3 and Fig. 4 present the distribution current and radiation pattern of the antenna respectively at three different positions for the frequencies 3.5 GHz and 5.8 GHz. As shown in Fig. 3, the direction of the current on the patch is always parallel to the longitudinal direction, and much current is concentrated at the ground plane, especially when $F_d = 12$ mm. This position of the feeding point may produce wider bandwidth due to the concentrated current around the patch and ground plane. From Fig. 3 and Fig. 4, the resultant distribution current and radiated field behaviors provide a clear physical understanding which is a useful design guideline for the antenna feeding structures. It is also interesting to notice that the pattern radiation of Fig. 4 agree well with the surface current distribution of the antenna. Hence,

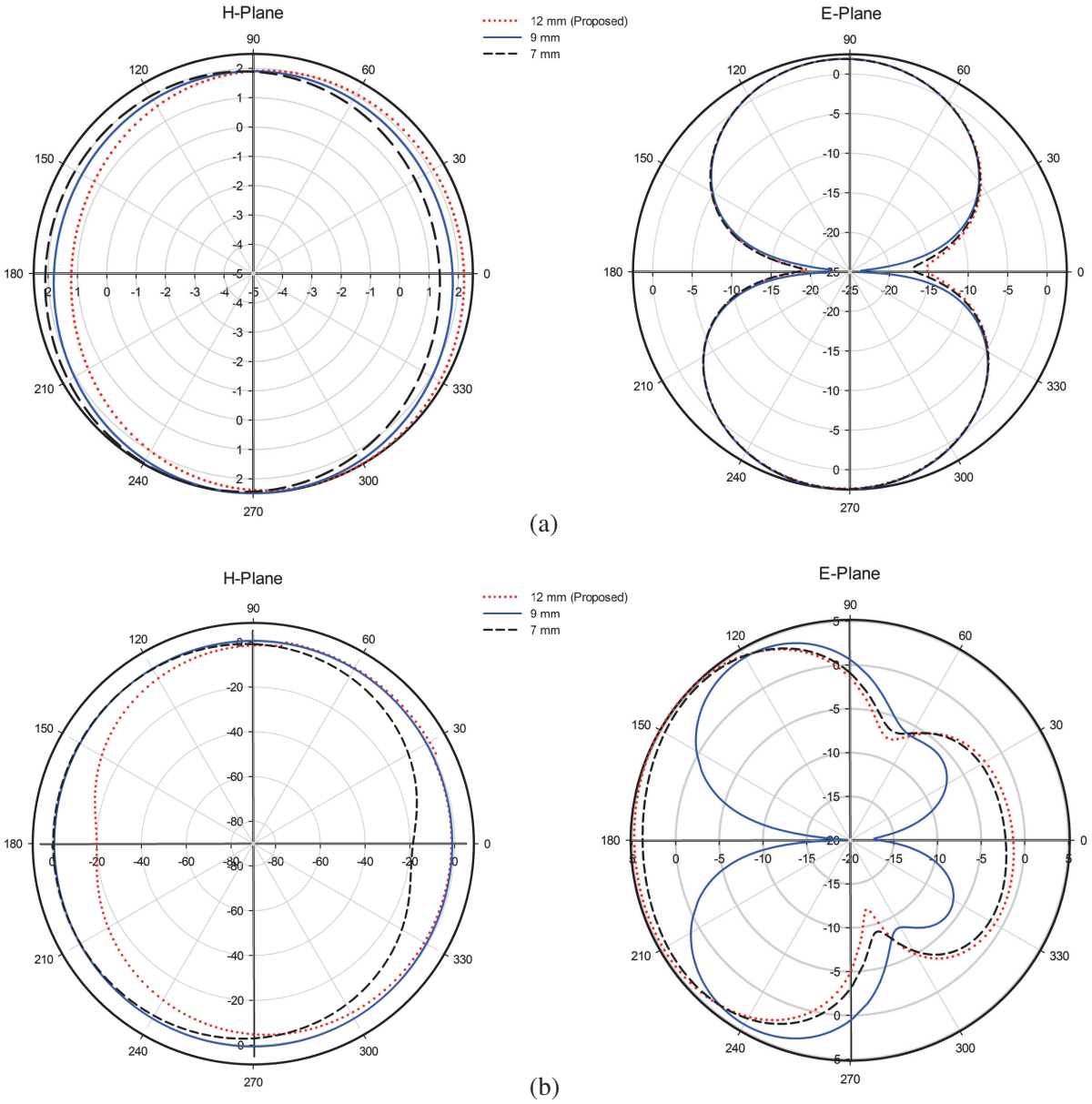

Figure 4. The radiation pattern for different positions of the feedline at H-plane and E-plane for: (a) 3.5 GHz, (b) 5.8 GHz.

the antenna remains omnidirectional regardless of the feedline's position. In order to demonstrate the antenna performance, we examine the gain, VSWR, and radiation pattern in polar coordinates. Fig. 5 shows variation of $VSWR$. As may be seen, the antenna exhibits a bandwidth of 9.1 GHz extending from 2.9 GHz $\sim$ 13 GHz with $VSWR \leq 2$. The value of $VSWR$ is less than 1.8 throughout the whole band, providing perfect matching between antenna and feeding system. A prototype of the antenna for high band frequencies has been fabricated and measured, and a reasonable agreement is achieved between the simulated and measured results [7].

For radar systems, such as UWB microwave imaging system for breast cancer detection, a moderate gain antenna is advantageous. Fig. 6 shows the peak gain versus frequency for the proposed antenna. The plotted gain reveals a high gain throughout the UWB frequency range. For the ISM band of central frequency of 5.8 GHz the peak gain is equal to 5.2 dBi which proves that the proposed antenna is a good candidate for cancer detection. The simplified equivalent circuit for the antenna is modeled as a parallel

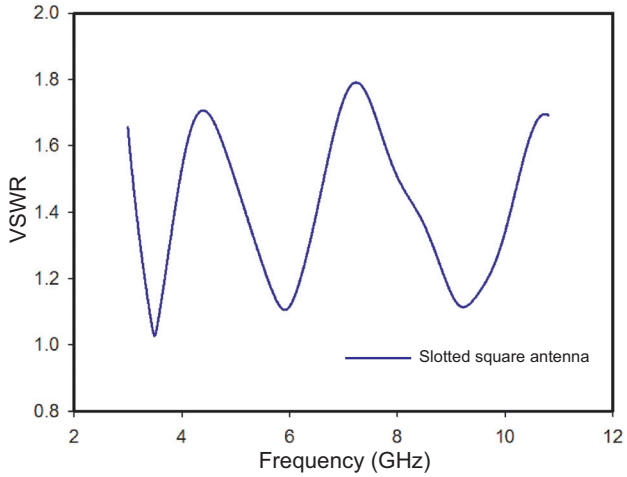

Figure 5. VSWR of the proposed antenna.

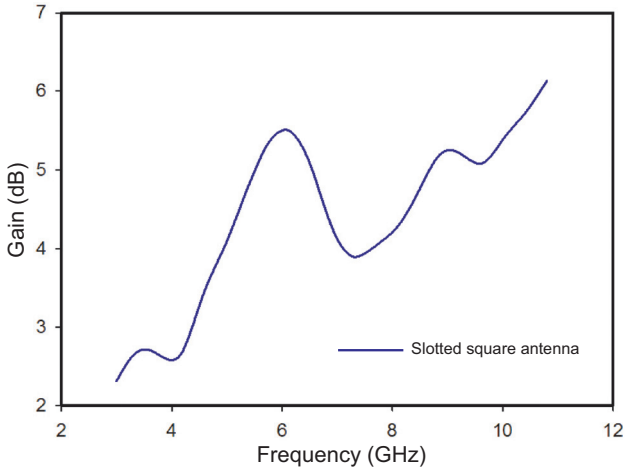

Figure 6. Gain of the proposed antenna.

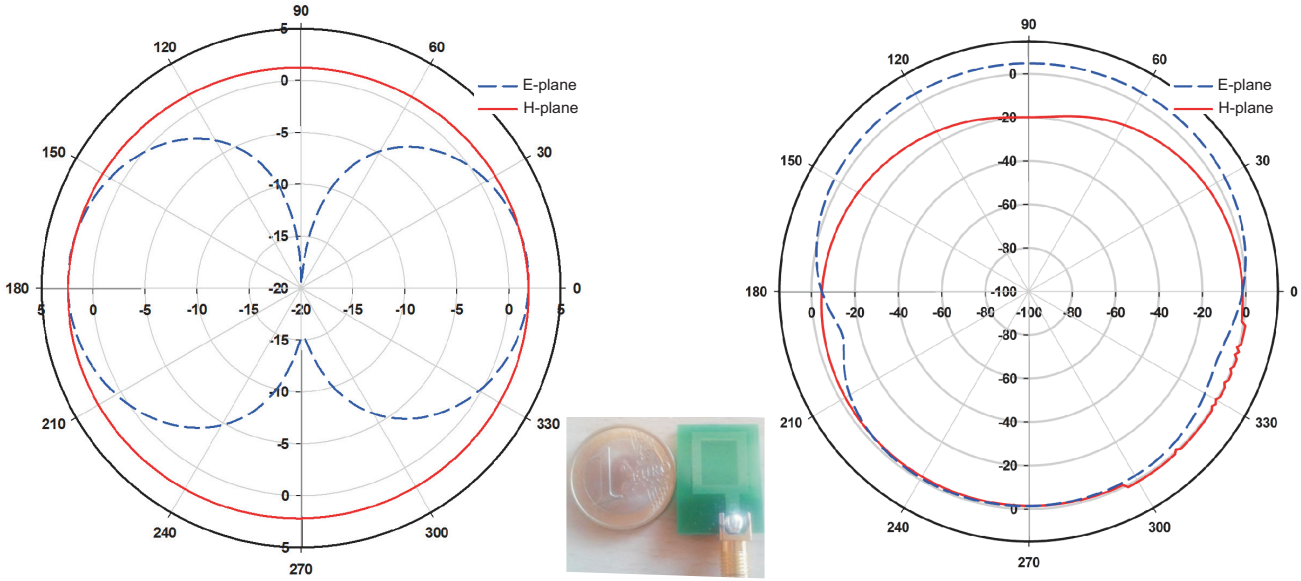

Figure 7. Radiation pattern at 3.5 GHz and 5.8 GHz for E-plane and H-plane respectively.

RLC circuit using resistors (R_i), inductors (L_i) and capacitors (C_i), for $i = 1, 2, \ldots, 5$, terminated by an impedance load of 50 Ω. More details can be found in our previous work [7]. The antenna performance can also be explored from the radiation patterns. As shown in Fig. 7 the radiation pattern is plotted for two different frequencies 3.5 GHz and 5.8 GHz. It is clear that the radiation behavior of the antenna is relatively omnidirectional, which means that the designed antenna is suitable for UWB application for breast tumor detection.

The current distributions on the rectangular ring as well as the feedline are calculated. Fig. 8 shows the current distributions on the rectangular ring shaped antenna at 5.8 GHz. The currents on the two vertical slot arms flow in the same direction and have a null in middle of the arms. It can be seen that the current is more exciting in strip line and wide slotted arms. Besides, the current density on the ground is more concentrated around the meandered slot than plane area, which can greatly improve the performance of the antenna.

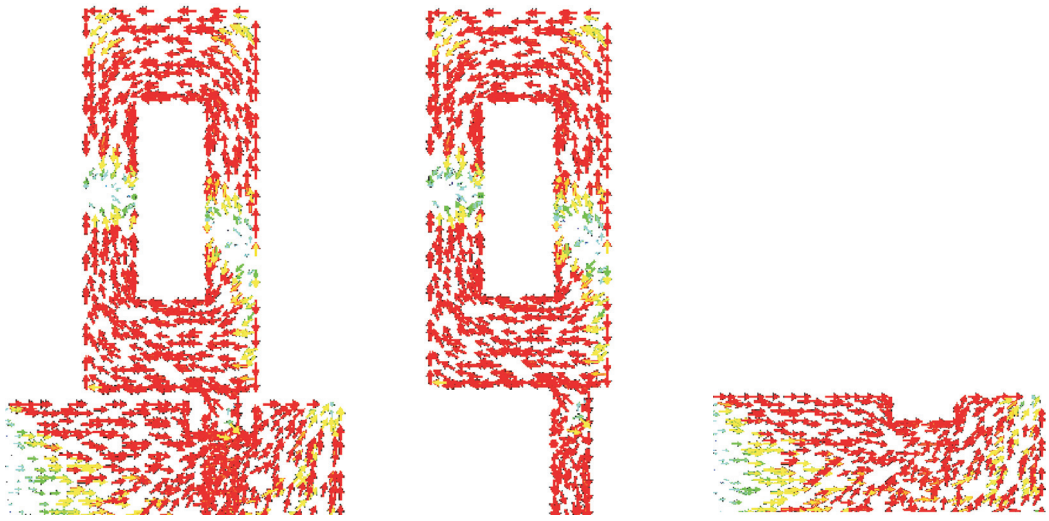

Figure 8. Current distribution of the proposed antenna at 5.8 GHz.

3.1. Specific Absorption Rate

The aim of this section is to implement the antenna designed previously on a breast-imaging tool for tumor cancer detection. The specific absorption rate is defined by the Institute of Electrical and Electronics Engineers ($IEEE$) as the time derivative of the incremental energy (dW) absorbed by an incremental mass (dm) contained in a volume element (dV) of a given mass density ρ. It is also defined as the power absorbed per mass of tissue. It is expressed as:

$$SAR = \frac{d}{dt}\left(\frac{dW}{dm}\right) = \frac{d}{dt}\left(\frac{dW}{\rho dV}\right) \tag{3}$$

In relation with electromagnetic energy, SAR can be calculated from the electric field in tissue as:

$$SAR = \frac{\sigma |E|^2}{\rho} \tag{4}$$

where SAR is the Specific Absorption Rate (W/kg), σ the conductivity (S/m) of the tissue, E the internal electric field (V/m), and ρ the mass density (kg/m^3). The limits of controlled and uncontrolled environments for local SAR over the whole-body SAR_{wb}, 1_g of tissue ($1G$), and 10_g of tissue ($10G$) are displayed in Table 3.

Table 3. SAR exposure limits in different environments.

	SAR_{wb}	SAR_{1g}	SAR_{10g}
Controlled environment	0.4	8	20
uncontrolled environment	0.08	1.6	4

3.2. Breast Cancer Detection System

In this paper we use a model of a hemispherical shape with the most common dimensions. Dielectric properties used to construct the model shown in Fig. 9 are presented in Table 1, where σ is the conductivity of the tissue and ε_r the dielectric permittivity. In the literature, the tumor size ranges from about 0.2 cm to 1.5 cm or more [13]. We use a spherical tumor with a radius of 5 mm. The developed model consists of a 50 mm radius hemisphere attached to a 2 mm layer that replicates the skin. The tumor of 5 mm is inserted in breast model at a location of $(5, 62, 40)$, and the model setup is shown in Fig. 9. The center of the patch antenna is placed at the origin, 10 mm away from the breast.

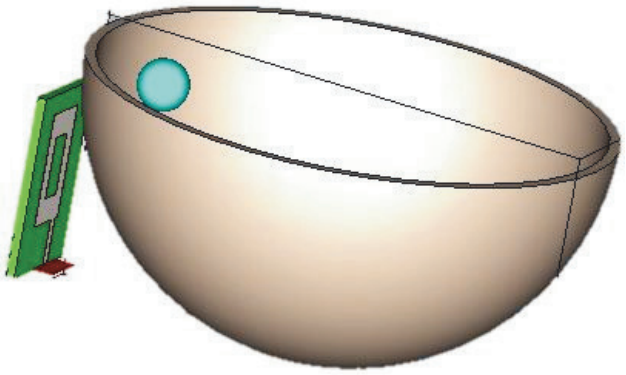

Figure 9. Heterogeneous breast model with 5 mm tumor of our abnormal breast.

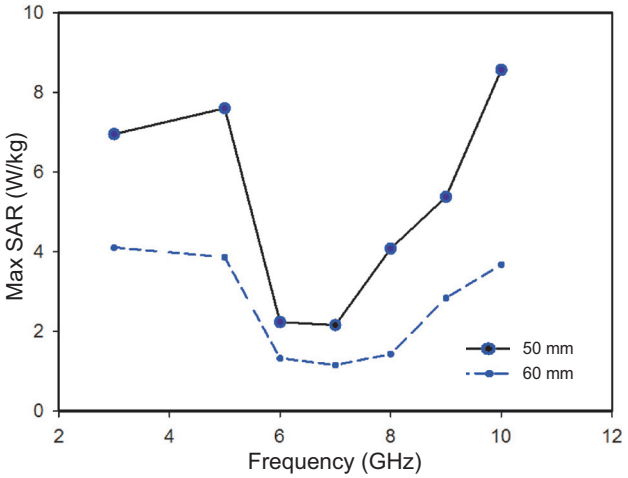

Figure 10. Maximum SAR values versus frequency two breast sizes.

3.3. Effect of Breast and Tumor Sizes on SAR

Figure 11 presents the simulated SAR distribution into the breast tissue. As may be seen, the simulation demonstrates significant absorbed energy from the tumor, while there is little power deposited in the skin due to its low electrical conductivity. The maximum SAR values for two sizes, 50 mm and 60 mm, of the abnormal breast at different frequencies are shown in Fig. 10. The tumor is placed at $(5, 62, 40)$ for both sizes. It is observed that when the mass of the breast increases, the maximum SAR value decreases for all frequencies. For example, the maximum SAR value for 50 mm breast at 5 GHz is 7.5990 W/kg. However at the same frequency, the maximum SAR value for 60 mm is 3.86 W/kg. The coordinates of the maximum value of SAR are summarized in Table 4 at frequencies from 3 GHz to 10 GHz, for different sizes of tumors 4 mm, 5 mm and 6 mm, placed inside a 50 mm breast at $(5, 62, 40)$. Simulation results demonstrate that the tumor size is a potential parameter for influencing the distribution of the max SAR values. At 5.8 GHz and for 4 mm tumor, the maximum value of SAR is 2.12225 W/kg. However, at the same frequency, the maximum value of SAR is 2.23352 W/kg for 5 mm and 4.52245 W/kg for 6 mm tumor.

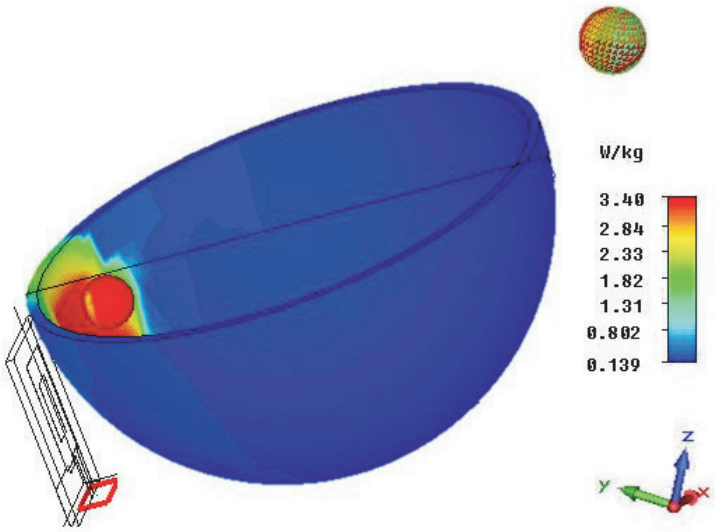

Figure 11. Simulated SAR distribution into the breast.

Table 4. Varying the size of tumor for 3 different sizes.

	tumor radius					
	4 mm		5 mm		6 mm	
Frequency (GHz)	Max SAR (W/kg)	Max at (x, y, z)	Max SAR (W/kg)	Max at (x, y, z)	Max SAR (W/kg)	Max at (x, y, z)
3.5	7.4613	5.48625, 55, 21.2755	6.94943	9.05, 53.7812, 19.5805	7.70509	9.68333, 54.1, 19.4808
5	6.79014	8.55, 56.3333, 42.3333	7.59901	8.41667, 60.1875, 35.7813	10.0915	7.33125, 58.75, 34.45
5.8	2.12225	10.45, 65.1419, 41.6667	2.23352	8.41667, 60.1875, 35.7813	4.52245	8.41667, 58.75, 35.5
7	1.22346	8.55, 56.3333, 42.3333	2.15738	8.41667, 60.1875, 35.7813	2.97489	7.33125, 58.75, 37.9
8	1.62572	11.5, 65.1419, 42.3333	4.07672	8.41667, 60.1875, 35.7813	3.48343	8.41667, 58.75, 35.5
9	5.54338	7.63875, 57.6667, 43.6667	5.37532	8.41667, 60.1875, 35.7813	5.36569	8.41667, 58.75, 35.5
10	2.99471	20.3958, 55.6667, 23.6764	8.56201	8.41667, 60.1875, 35.7813	5.31996	9.05, 60.1, 35.5

3.4. Tumor Location Effects

Table 5 shows the detection of a 5 mm tumor at 5.8 GHz according to the maximum value of SAR. The tumor is located at five different positions. It is observed that the coordinates of maximum value of SAR actually point to the position of the tumor.

Table 5. Actual position of tumor versus detected position of tumor at 5.8 GHz.

Actual Position of Tumor at (w, y, z)	Detected Position of Tumor at (x, y, z)
(10, 45, 25)	(7.55, 45.0699, 29.6532)
(5, 62, 40)	(8.41667, 60.1875, 35.7813)
(13, 53, 27)	(12.55, 56.4375, 31.5313)
(17, 58, 39)	(14.4625, 60.1875, 34.4688)

4. SYSTEM DESIGN WITH SKIN AND FAT

In order to obtain a breast model closer to reality, we introduce a 48 mm fat layer into the breast together with the skin layer discussed earlier. The fat tissue parameters are: $\varepsilon_r = 22.57$ and $\sigma_s = 0.31$ (S/m). The new breast model is shown in Fig. 12. Table 6 summarizes the values and coordinates of total SAR and maximum SAR in the new breast model at different frequencies. The tumor is located into the breast at $(10, 45, 25)$. Results indicate that the coordinates of maximum value of SAR actually point to the position of the tumor.

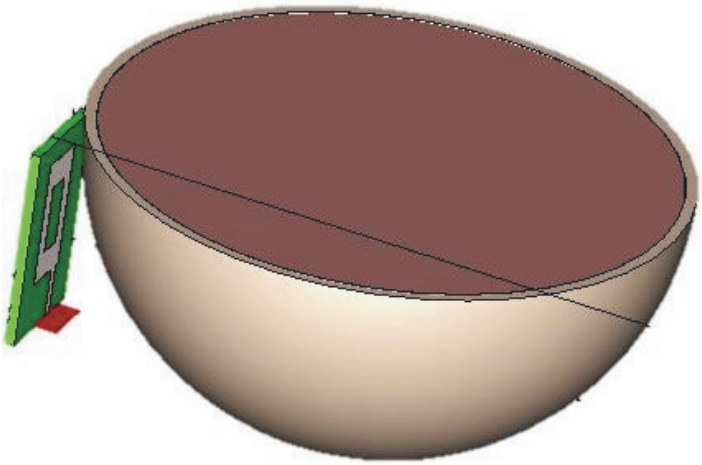

Figure 12. New breast model.

Table 6. Values and coordinates of 1-G averaged local SAR in breast with tumor.

Frequency	Total SAR (W/kg)	Max SAR (W/kg)	Max at (x, y, z)
3.5	10.4696	28.6137	9.68333, 45.8333, 24.25
5.8	2.96485	20.41	7.55, 45.0699, 29.6532
7	0.93778	5.19465	8.41667, 45.0699, 29.6532
8	1.82361	9.91655	8.41667, 45.0699, 29.6532
9	2.57191	10.8296	7.55, 45.0699, 29.6532
10	2.57323	10.9775	6.36345, 47.1667, 24.25

Table 7 shows the detection of the 5 mm tumor at 5.8 GHz according to the maximum value of SAR. The tumor is placed at three locations. From simulation results, it can be observed that the tumor is detected by the antenna at all positions.

Table 7. Actual position of tumor versus detected position of tumor at 5.8 GHz.

Tumor actual position at (w, y, z)	Detected position of tumor at (x, y, z)
(20, 45, 20)	(20.4687, 45.4688, 19.5313)
(17, 37, 12)	(17.45, 37.4688, 11.2187)
(−5, 40, 30)	(−4.53125, 39.5312, 29.5313)

5. CONCLUSION

This paper presents a novel method for locating a tumor using a new breast model system based on a UWB antenna. The antenna performs reasonably well in terms of VSWR, gain and radiation pattern. To test the efficiency of our system, a breast model with dielectric properties of a human breast is designed. Simulation of the rectangular ring shaped antenna in our system demonstrates that the breast tumor can be detected by considering the difference of the power absorbed in normal tissue and malignant tissue. The coordinates for maximum value of SAR can be used as an indication for locating a tumor.

REFERENCES

1. Adnan, S., R. A. Abd-Alhameed, M. Usman, C. H. See, J. M. Noras, and M. B. Child, "Simulation and experimental measurements for near field imaging," *PIERS Proceedings*, 433–437, Kuala Lumpur, Malaysia, March 27–30, 2012.
2. Santorelli, A. and M. Popovi, "SAR distribution in microwave breast screening: Results with TWTLTLA wideband antenna," *IEEE Intelligent Sensors, Sensor Networks and Information Processing*, 11–16, 2011.
3. Shahira Banu, M. A., S. Vanaja, and S. Poonguzhali, "UWB microwave detection of breast cancer using SAR," *International IEEE Conference on Energy Efficient Technologies for Sustainability (ICEETS)*, 113–118, Nagercoil, Inde, Apr. 2013.
4. Lazebnik, M., D. Popovic, L. McCartney, et al., "A large-scale study of the ultra-wideband microwave dielectric properties of normal, benign and malignant breast tissues obtained from cancer surgeries," *Physics in Medicine and Biology*, Vol. 52, No. 20, 6093–6115, 2007.
5. Tiang, S. S., M. S. Hathal, N. S. Nik Anwar, M. F. Ain, and M. Z. Abdullah, "Development of a compact wide-slot antenna for early stage breast cancer detection featuring circular array," *International Journal of Antennas and Propagation*, Vol. 2014, Article ID 309321, 11 pages, 2014.
6. Ojaroudi, N., M. Ojaroudi, and Y. Ebazadeh, "UWB/Omni-directional microstrip monopole antenna for microwave imaging applications," *Progress In Electromagnetics Research C*, Vol. 47, 139–146, 2014.
7. Akrou, L., O. Aghzout, H. Silva, and M. Essaaidi, "Design of compact multiband antenna with band-rejection features for mobile broadband satellite communications," *Progress In Electromagnetics Research C*, Vol. 68, 95–106, 2016.
8. Chaudhary, S. S., R. K. Mishra, A. Swarup, and J. M. Thomas, "Dielectric properties of normal and malignant human breast tissues at radiowave and microwave frequencies," *Indian J. Biochem. Biophys.*, Vol. 21, 76–79, 1984.
9. Joines, W. T., Y. Z. Dhenxing, and R. L. Jirtle, "The measured electrical properties of normal and malignant human tissues from 50 to 900 MHz," *Med. Phys.*, Vol. 21, 547–550, 1994.
10. Zastrow, E., S. K. Davis, M. Lazebnik, F. Kelcz, B. D. Van Veen, and S. C. Hagness, "Database of 3D grid-based numerical breast phantoms for use in computational electromagnetics simulations," http://uwcem.ece.wisc.edunhome.htm.
11. Zahirul Alam, A. H. M., I. Md. Rafiqul, and S. Khan, "Tuning fork UWB antenna with unsymmetrical feed line," *PIERS Proceedings*, 1457–1460, Moscow, Russia, August 19–23, 2012.
12. Ali, J. K., M. T. Yassen, M. R. Hussan, and M. F. Hasan, "A new compact ultra wideband printed monopole antenna with reduced ground plane and band notch characterization," *PIERS Proceedings*, 1531–1536, Kuala Lumpur, Malaysia, March 27–30, 2012.
13. AlShehri, S. A. and S. Khatun, "UWB imaging for breast cancer detectionusing neural network," *Progress In Electromagnetics Research C*, Vol. 7, 79–83, 2009.